kidney and dialysis

MDPI

Case Report

Prolonged Neonatal Continuous Kidney Replacement Therapy Complicated by Recurrent Circuit Clotting and Persistent Thrombocytopenia: Morphological Assessment by Scanning Electron Microscopy

Atsu Todo [1], Mika Sakaguchi [2,*], Shota Torama [1], Takumi Ito [1], Toshikazu Yogai [1], Hitoshi Katsurao [1], Yoshifumi Masuda [1], Kenichi Nakano [1], Masanori Yoshioka [1], Keisuke Sugimoto [3] and Shuji Arima [2]

[1] Department of Clinical Engineering, Kindai University Hospital, Osaka 590-0197, Japan; atsu.todo@med.kindai.ac.jp (A.T.); torama@med.kindai.ac.jp (S.T.); takumi.kindai@med.kindai.ac.jp (T.I.); yo-gaitoshi@med.kindai.ac.jp (T.Y.); katurao.ce@med.kindai.ac.jp (H.K.); ce.masuda@med.kindai.ac.jp (Y.M.); cenakano@med.kindai.ac.jp (K.N.); cemeyoshioka@med.kindai.ac.jp (M.Y.)

[2] Department of Nephrology, Kindai University Hospital, Osaka 590-0197, Japan; shuarima@med.kindai.ac.jp

[3] Department of Pediatrics, Kindai University Faculty of Medicine, Osaka 590-0197, Japan; ksugimo@med.kindai.ac.jp

* Correspondence: msakaguchi@med.kindai.ac.jp; Tel.: +81-72-288-7222

Abstract

Neonatal continuous kidney replacement therapy (CKRT) is complicated by technical constraints, circuit clotting, and thrombocytopenia. We report a term female neonate with severe birth asphyxia, disseminated intravascular coagulation, and acute kidney injury who required prolonged CKRT with recurrent circuit clotting and repeated platelet transfusions. CKRT was initiated on day of life (DOL) 5, and persistent anuria prompted transfer to a specialized pediatric center for consideration of peritoneal dialysis on DOL 38. Three intentionally selected circuits were examined qualitatively by scanning electron microscopy (SEM): a cellulose triacetate membrane with post-dilution on ACH-Σ, and polyarylethersulfone membranes with combined pre- and post-dilution on Prismaflex at pre-blood-pump (PBP) flow rates of 100 and 300 mL/h. Circuit durations were 5 h 30 min, 6 h 40 min, and 7 h 53 min, respectively. Retrieved membranes and pump-tubing surfaces showed blood cell-like structures, platelet-like aggregates, and fibrin-like networks. Adherent structures appeared relatively sparse in selected images from the PBP 300-mL/h circuit despite its longer exposure. These morphology-based, nonquantitative observations cannot establish the effects of individual treatment factors or a causal relationship between CKRT and thrombocytopenia. Further standardized studies are needed to investigate blood–material interactions during neonatal CKRT.

Keywords: neonatal acute kidney injury; continuous kidney replacement therapy; circuit clotting; scanning electron microscopy; blood–material interactions; dilution strategy

Academic Editor: Francesco Locatelli

Received: 28 September 2026
Revised: 23 November 2026
Accepted: 25 November 2026
Published: 27 November 2026

Copyright: © 2026 by the author. Licensee MDPI, Basel, Switzerland. This article is an open access article distributed under the terms and conditions of the Creative Commons Attribution (CC BY) license.

1. Introduction

Acute kidney injury (AKI) is a frequent and serious complication of severe birth asphyxia and neonatal encephalopathy [1–3]. It may result from renal hypoperfusion, ischemia–reperfusion injury, systemic inflammation, coagulation abnormalities, and tubular

injury [1]. Continuous kidney replacement therapy (CKRT) may be required in neonates with severe fluid overload, electrolyte or acid–base disturbances, or persistent oliguria or anuria [1,4]. However, neonatal CKRT is technically challenging because of the small circulating blood volume, relatively large extracorporeal circuit volume, low blood flow rates, difficulties in temperature control, and risks of hemodynamic instability and circuit clotting [4,5].

Peritoneal dialysis (PD) is an established kidney replacement modality for neonatal AKI; modality selection depends on the clinical condition, local expertise, and available resources [1,6]. Infant-specific extracorporeal systems, including CARPEDIEM and NIDUS, have been developed to address the challenges of extracorporeal volume and fluid removal in small infants, although availability varies between centers [7,8].

We previously reported a structured neonatal CKRT management approach incorporating blood priming, electrolyte correction, blood warming, and divided administration of nafamostat mesylate [5]. Nevertheless, thrombocytopenia, bleeding, and recurrent circuit clotting remain important concerns, particularly during prolonged therapy [4,5]. Vascular-access characteristics may also substantially affect circuit survival in pediatric CKRT [9].

Contact between blood and artificial surfaces results in rapid protein adsorption, followed by platelet and leukocyte adhesion and activation, which may promote coagulation and fibrin deposition [10,11]. These interactions may affect membrane biocompatibility and circuit patency. Membrane material and dilution mode may influence cellular deposition and local hemoconcentration [10–12]. However, direct morphological evidence of these interactions during neonatal CKRT remains limited.

We report a term neonate with severe birth asphyxia, disseminated intravascular coagulation, thrombocytopenia, and severe AKI requiring prolonged CKRT. Recurrent circuit clotting and persistent thrombocytopenia requiring repeated platelet transfusions occurred during treatment with different membrane materials and dilution configurations. Retrieved hemofilters and selected circuit components were examined by scanning electron microscopy (SEM). This report provides a descriptive, exploratory account of the clinical course and surface morphology; it does not isolate the effects of membrane material, platform, dilution mode, or other treatment conditions.

2. Case Presentation

2.1. Perinatal History and Initial Clinical Course

A female infant was born vaginally at 41 weeks and 3 days of gestation, with a birth weight of 2978 g. Labor was induced because of recurrent fetal bradycardia. Apgar scores were 0 at both 1 and 5 min. No spontaneous crying or detectable heartbeat was observed immediately after birth, and resuscitation was initiated with positive-pressure ventilation, supplemental oxygen, and chest compressions. Although the heart rate transiently recovered, severe bradycardia recurred, requiring endotracheal intubation, repeated epinephrine administration, intravenous fluid resuscitation, and sodium bicarbonate before transfer to our neonatal intensive care unit.

Venous blood gas analysis approximately 1 h after birth showed severe mixed acidosis, with a pH of 6.874, pCO_2 of 100.5 mmHg, HCO_3^- of 18.5 mmol/L, and base excess of −15 mmol/L. The infant exhibited profound pallor, hypotonia, absent sucking and grasp reflexes, weak pupillary responses, and severe circulatory instability. The lowest hemoglobin concentration during the initial resuscitation period was 3.8 g/dL. Fetomaternal transfusion was suspected on the basis of the profound anemia and perinatal course, although it was not definitively established. A confirmatory Kleihauer–Betke test or maternal flow-cytometric assessment could not be verified in the available records; fetomaternal hemorrhage therefore remains a suspected diagnosis.

https://doi.org/10.3390/kidneydial6040074

Therapeutic hypothermia was initiated within 6 h after birth and continued for 72 h, followed by controlled rewarming. Severe birth asphyxia and hypoxic–ischemic encephalopathy were diagnosed.

Disseminated intravascular coagulation (DIC) was accompanied by bleeding from vascular-access sites, coagulation abnormalities, and severe thrombocytopenia. Treatment included red blood cell, fresh frozen plasma, and platelet transfusions and recombinant human soluble thrombomodulin. Exchange transfusion was performed on day of life (DOL) 4 because of persistent coagulation abnormalities and severe systemic illness. Selected perinatal and clinical findings are summarized in Table 1.

Table 1. Perinatal characteristics and clinical timeline.

Variable	Finding
Day-of-life convention	Birth = DOL 0
Gestational age	41 weeks + 3 days
Sex	Female
Birth weight	2978 g
Apgar score	0 at 1 min; 0 at 5 min
Venous blood gas at approximately 1 h	pH 6.874; pCO_2 100.5 mmHg; HCO_3^- 18.5 mmol/L; base excess −15 mmol/L
Lowest hemoglobin during initial resuscitation	3.8 g/dL
Fetomaternal transfusion	Suspected
Therapeutic hypothermia	Initiated within 6 h after birth; continued for 72 h
Disseminated intravascular coagulation	Present during the early clinical course
Exchange transfusion	DOL 4
Admission laboratory sample	DOL 0
Kidney ultrasound	Left grade II hydronephrosis, subsequently improved
CKRT initiation	DOL 5
Principal indications for CKRT	Persistent near-anuria, progressive fluid overload, and pulmonary edema
Persistent complete anuria	From DOL 26
Transfer	DOL 38
Early urine-output course	Very small intermittent amounts; near-anuria despite diuretic therapy
Right femoral dialysis catheter	A 6-Fr double-lumen catheter was documented in the right femoral vein; no subsequent catheter replacement was verified in the reviewed records.
Lowest platelet count in the available laboratory series	14×10^9/L on DOL 12

DOL, day of life; CKRT, continuous kidney replacement therapy. Birth was designated DOL 0. Clinical events and laboratory values were obtained from the available medical records. The platelet nadir represents the lowest recorded value in the available laboratory series. The lowest hemoglobin concentration during initial resuscitation was 3.8 g/dL; the admission laboratory sample obtained after resuscitation and blood-product administration showed a hemoglobin concentration of 7.5 g/dL.

2.2. Development of Acute Kidney Injury and Initiation of CKRT

Despite circulatory support with repeated blood product transfusions, vasoactive agents, corticosteroids, and diuretic therapy, urine output remained minimal and generalized edema progressively worsened. The kidney injury was considered primarily related to prolonged circulatory failure and renal hypoperfusion associated with severe birth asphyxia and profound anemia.

During the first several days of life, marked generalized edema developed, accompanied by pulmonary edema and increasing respiratory support requirements. Despite improvement in blood pressure and repeated administration of furosemide, urine output remained extremely low. Left grade II hydronephrosis was noted on ultrasonography but subsequently showed improvement and was not considered sufficient to explain the severe kidney dysfunction. Other ultrasound findings included preserved bilateral renal blood flow, normal kidney size, and no obvious sonographic evidence of renal infarction. A detailed renal Doppler report could not be verified in the available records. The available ultrasound findings did not definitively exclude cortical necrosis, renal vascular thrombosis, or other intrinsic kidney diseases. Based on the perinatal course, hypoxic–ischemic injury was considered the most likely cause of AKI.

On DOL 4, exchange transfusion was performed for persistent DIC and severe systemic illness. Although coagulation parameters subsequently improved, oliguria persisted. At CKRT initiation, the blood urea nitrogen concentration was 65 mg/dL and serum creatinine was 3.55 mg/dL. The infant remained nearly anuric, with progressive generalized and pulmonary edema. CKRT in continuous hemodiafiltration mode was therefore initiated on DOL 5 because of persistent near-anuria, progressive generalized and pulmonary edema, and increasing azotemia.

Serum creatinine decreased during CKRT, but sustained kidney recovery was not achieved. Only small amounts of urine were intermittently observed during the early clinical course, and complete anuria persisted from DOL 26 onward. Selected laboratory findings at admission and CKRT initiation are shown in Table 2.

CKRT was selected initially for severe fluid overload and pulmonary edema while the treating team monitored for possible kidney recovery, consistent with local practice and available expertise. This was an institutional treatment decision; PD was not considered intrinsically unsuitable for potentially reversible AKI. CARPEDIEM and NIDUS were not available at our hospital, where existing blood purification systems were used with neonatal or pediatric circuits and hemofilters.

Table 2. Laboratory findings at admission, CKRT initiation, and during follow-up.

A. Laboratory Findings at Admission and on the Day of CKRT Initiation			
Variable	**Unit**	**Admission**	**CKRT Initiation Day**
		DOL 0	**DOL 5**
C-reactive protein	mg/dL	0	0.12
Sodium	mmol/L	153	132
Potassium	mmol/L	4.9	5
Chloride	mmol/L	93	84
Blood urea nitrogen	mg/dL	8	65
Serum creatinine	mg/dL	0.69	3.55
Uric acid	mg/dL	8.1	18.5
Total protein	g/dL	2.2	4.2
Albumin	g/dL	1.4	2.5
Aspartate aminotransferase	U/L	98	217
Alanine aminotransferase	U/L	29	100
Lactate dehydrogenase	U/L	588	2057
White blood cell count	$\times 10^9$/L	12.97	18.15
Hemoglobin	g/dL	7.5	7.9
Hematocrit	%	24.6	23
Platelet count	$\times 10^9$/L	144	18
Activated partial thromboplastin time	s	120.6	30.9
Fibrinogen	mg/dL	48	118

B. Platelet Counts and Coagulation Measurements by Day of Life				
DOL	**PLT ×10⁹/L**	**aPTT s**	**aPTT/Control ratio**	**Fibrinogen mg/dL**
0	144	120.6	4.17	48
1	73	82.2	2.84	13
2	22	61.1	2.11	78
3	36	44.2	1.53	143
4	17	33.9	1.17	170
5	18	30.9	1.07	118
6	32	41.7	1.44	97
7	58	52	1.80	93
8	23	73.3	2.54	201
9	17	66.4	2.30	157
10	19	66.4	2.30	105
11	17	65.9	2.28	72
12	14	59.9	2.07	43
13	35	67.5	2.34	61
14	48	63.5	2.20	61
15	105	71	2.46	63
16	141	39.5	1.37	73
17	65	77.5	2.68	53
18	64	64.3	2.22	67
19	86	61.5	2.13	97
20	105	60.2	2.08	119
21	94	53.4	1.85	89
24	62	58.9	2.04	51
28	67	55.5	1.92	64
37	72	44.7	1.55	145

(A) Admission samples were collected after resuscitation and administration of blood products. Samples on DOL 5 were collected on the day of CKRT initiation, but the timing of sampling relative to circuit connection could not be confirmed; (B) DOL 0 denotes birth. Morning laboratory results are shown for each listed DOL, except for the admission sample on DOL 0, which was obtained in the afternoon. Only available results are listed; omitted days do not indicate normal values. PLT, platelet count. PLT and coagulation results correspond to the same recorded sampling timestamps. The aPTT control value was 28.9 s for all measurements; aPTT/control ratios were calculated from this value and rounded to two decimal places. These are routine patient samples, not confirmed circuit-start or paired pre-/post-filter measurements. Actual ACT measurements were unavailable; approximately 200 s was an institutional management target. No blood samples were collected on DOL 38, the day of transfer.

2.3. CKRT Delivery, Vascular Access, and Anticoagulation

CKRT was initiated on DOL 5 using an ACH-Σ system (Asahi Kasei Medical Co., Ltd., Tokyo, Japan), with a dialysis catheter used for vascular access from the outset. During the treatment course, a 6-Fr double-lumen dialysis catheter in the right femoral vein was documented. The earliest access history could not be reconstructed completely. At initiation, withdrawal difficulty required a reduction in blood flow from 25 to 20 mL/min. On DOL 32, a withdrawal pressure of approximately −180 mmHg with the usual connection prompted reversal of the catheter connections. Access recirculation was considered clinically but its rate was not measured. These access observations were not conclusively linked to the three SEM specimens.

Because the extracorporeal volume was large relative to the infant's circulating blood volume, red blood cells and fresh frozen plasma were used for blood priming. Priming

blood was circulated and dialyzed before patient connection to adjust electrolyte composition, bicarbonate concentration, and hematocrit. The same general priming approach was used with both platforms, although the mixture of blood products, use of recovered circuit blood, and preconnection dialysis settings could vary between exchanges. Blood flow during patient treatment was generally 20–26 mL/min; high preconnection priming flows were separate from patient-treatment settings.

Nafamostat mesylate was used for CKRT anticoagulation. The preparation contained 50 mg in 50 mL of 5% dextrose solution (1 mg/mL), administered by syringe pump. The initial infusion rate was 2 mL/h (2 mg/h). The institutional usual starting dose was approximately 0.5 mg/kg/h; an actual weight-adjusted dose for each later circuit could not be calculated without contemporaneous body weight. The clinical monitoring goals were an activated clotting time (ACT) of approximately 200 s and an activated partial thromboplastin time (aPTT) of approximately 1.5–2 times the normal control value. Dose adjustments considered ACT/aPTT prolongation, bleeding risk, and circuit findings; these were clinical goals rather than consistently attained values. Actual ACT measurements were unavailable in the reviewed records; the ACT target therefore does not establish the achieved anticoagulation level. Available aPTT values and their ratios to the recorded control of 28.9 s, together with fibrinogen values, are presented in Table 2.

For SEM circuit A, nafamostat was divided between a port on the withdrawal limb before the blood pump (1.0 mL/h) and the venous chamber (0.3 mL/h). For circuits B and C, 1.3 mL/h was infused between the blood pump and the hemofilter through a separate syringe line, not through the PBP replacement-fluid line. Thus, the total dose was the same at 1.3 mg/h, but the fraction delivered upstream of the hemofilter and its delivery relative to the blood pump differed between platforms. Nafamostat delivery sites were the same in B and C.

Nafamostat was the institutional preference because of concern about bleeding, including intracranial hemorrhage, with systemic heparin in this setting. Heparin was not the CKRT anticoagulant, although heparin catheter locking was documented. Citrate use for CKRT anticoagulation is off-label in Japan [13], and regional citrate anticoagulation was not available as a treatment option at our institution.

Circuit duration varied substantially. Some circuits required replacement after approximately 20–26 h because of visible clot formation or increased circuit pressure, whereas others remained functional for approximately 48–67 h. CKRT was temporarily interrupted during selected circuit exchanges to assess kidney recovery and reduce transfusion requirements; however, worsening fluid balance required repeated resumption of CKRT.

The pressure thresholds used as practical indicators of possible circuit clotting and need for exchange were an inlet pressure of 250 mmHg, a venous pressure of 200 mmHg, and a transmembrane pressure (TMP) of 150 mmHg. Treatment was discontinued or the circuit was exchanged when an alarm could not be resolved and continuation was impracticable. Reaching a threshold alone was not treated as proof of membrane thrombosis.

2.4. Thrombocytopenia and Changes in Treatment Conditions

Although the coagulation abnormalities associated with disseminated intravascular coagulation (DIC) gradually improved, severe thrombocytopenia persisted. Platelet transfusions were repeatedly administered to maintain the platelet count at approximately 50 × 10^9/L and reduce bleeding risk.

Maternal anti-SS-A and anti-SS-B antibodies, antiplatelet antibodies, platelet-associated immunoglobulin G, and antibodies associated with heparin-induced thrombocytopenia were negative. Testing for human platelet antigen incompatibility or a formal

assessment for neonatal alloimmune thrombocytopenia could not be verified in the available records.

Platelet counts fluctuated during CKRT and were described clinically as relatively better maintained during selected treatment interruptions (Figure 1). However, severe DIC, continuing critical illness, transfusions, and the reasons for interruption confounded this temporal association. Routine laboratory sampling was generally performed in the morning and late afternoon; morning laboratory results are summarized by day of life (DOL) in Table 3B. Samples were not paired with pre- and post-filter measurements and were not obtained at standardized intervals after transfusion.

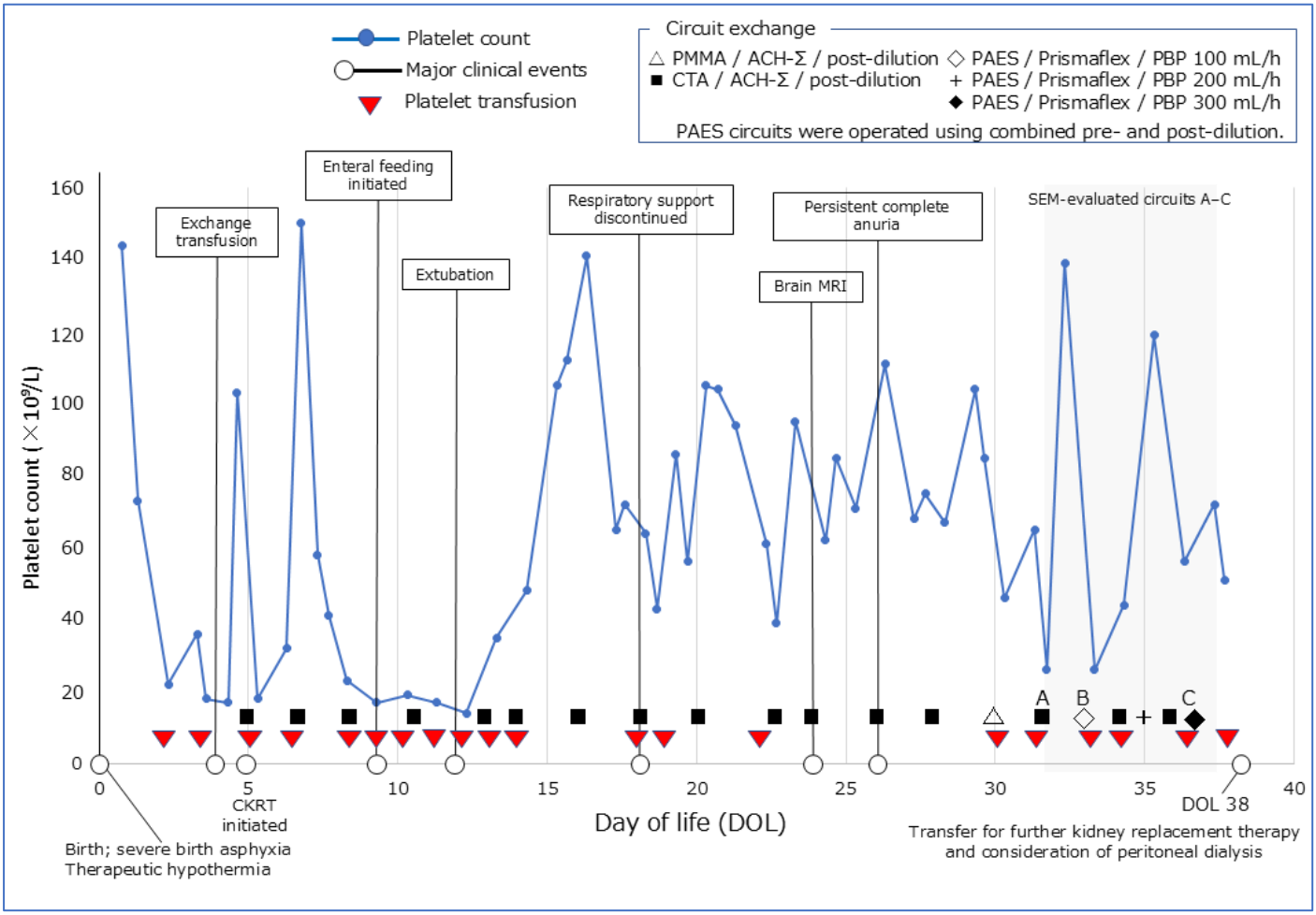


Figure 1. Clinical course, platelet counts, platelet transfusions, circuit exchanges, and major clinical events during neonatal CKRT**.** The blue line with circles shows platelet counts (×10⁹/L). Red inverted triangles indicate platelet-transfusion episodes identified from the available electronic blood-product records and summarized in Supplementary Table S1. Open circles indicate major clinical events. Circuit exchanges are indicated by condition-specific symbols: open triangles, PMMA with post-dilution on ACH-Σ; filled squares, CTA with post-dilution on ACH-Σ; open diamonds, PAES with PBP flow of 100 mL/h on Prismaflex; plus signs, PAES with PBP flow of 200 mL/h on Prismaflex; and filled diamonds, PAES with PBP flow of 300 mL/h on Prismaflex. PAES circuits used combined pre- and post-dilution. Labels A, B, and C identify the SEM-evaluated circuits used on DOL 32, 33, and 37, respectively; their operating conditions are summarized in Table 3A. The shaded area indicates the period during which these circuits were used. Platelet measurements were obtained during routine clinical care and were not collected at standardized intervals after transfusion. CKRT, continuous kidney replacement therapy; DOL, day of life; MRI, magnetic resonance imaging; SEM, scanning electron microscopy; PMMA, polymethyl methacrylate; CTA, cellulose triacetate; PAES, polyarylethersulfone; PBP, pre-blood pump.

https://doi.org/10.3390/kidneydial6040074

Table 3. Operating conditions and available laboratory context for the SEM circuits.

A. Circuit Operating Conditions			
Characteristic	**Circuit A**	**Circuit B**	**Circuit C**
DOL of circuit use	32	33	37
CKRT system	ACH-Σ	Prismaflex	Prismaflex
Hemofilter	UT-03 Seco	HF20	HF20
Membrane material	CTA	PAES	PAES
Dilution configuration	Post-dilution	Combined pre/post	Combined pre/post
Blood flow, mL/min	26	26	26
Dialysate flow, mL/h	100	0	0
PBP replacement flow, mL/h	0	100	300
Post-filter replacement flow, mL/h	100	100	60
Patient net fluid removal, mL/h	25	25	25
Calculated nominal membrane ultrafiltration, mL/h	125	225	385
Calculated concentration ratio, %	8.0	13.6	20.7
Nafamostat concentration, mg/mL	1.0	1.0	1.0
Total nafamostat, mg/h	1.3	1.3	1.3
Nafamostat infusion site and rate	Before blood pump: 1.0 mg/h; venous chamber: 0.3 mg/h	Between blood pump and filter: 1.3 mg/h	Between blood pump and filter: 1.3 mg/h
Circuit duration	5 h 30 min	6 h 40 min	7 h 53 min
Termination indication	Pressure-alarm limit; exact alarm unverified	Pressure-alarm limit; exact alarm unverified	Pressure-alarm limit; exact alarm unverified

B. Patient Laboratory Values by Day of Life During the Later Sampling Period			
DOL	**PLT (×10⁹/L)**	**Hct (%)**	**Hb (g/dL)**
29	104	25.0	8.5
30	46	25.0	8.8
31	65	25.1	8.7
32	139	25.2	8.7
33	26	27.2	9.4
34	44	27.8	9.7
35	119	26.6	9.2
36	56	25.3	8.7
37	72	24.7	8.8

(A) CKRT, continuous kidney replacement therapy; CTA, cellulose triacetate; PAES, polyarylethersulfone; PBP, pre-blood pump. Nominal membrane ultrafiltration was calculated as PBP replacement flow + post-filter replacement flow + patient net fluid removal. Concentration ratio (%) was calculated as 100 × nominal membrane ultrafiltration flow/(blood flow + PBP replacement flow), with all flow rates expressed in mL/h. Dialysate and anticoagulant syringe flows were excluded. These values were derived from prescribed settings rather than measured fluid volumes. Concentration ratio is distinct from plasma-based filtration fraction. Nafamostat was administered at a concentration of 1 mg/mL, with a total dose of 1.3 mg/h in each circuit. In circuits B and C, it was infused through a separate syringe line between the blood pump and filter, not through the PBP line. Filtration fraction was not calculated because hematocrit at the start of each circuit could not be verified. Available aPTT and fibrinogen measurements are presented in Table 2B. Actual ACT measurements were unavailable; approximately 200 s was an institutional management target. (B) Morning laboratory results are shown for each listed DOL. DOL, day of life; PLT, platelet count; Hct, hematocrit; Hb, hemoglobin. Coagulation measurements are presented in Table 2B. These are routine patient samples, not confirmed circuit-start, paired pre-/post-filter, or standardized post-transfusion measurements. No blood samples were collected on DOL 38, the day of transfer.

https://doi.org/10.3390/kidneydial6040074

A cellulose triacetate (CTA) hemofilter (UT-03 Seco; Nipro Corporation, Osaka, Japan) was used for most sessions. A polymethyl methacrylate (PMMA) hemofilter (CH-0.3W; Toray Industries, Inc., Tokyo, Japan) was used from DOL 29 to DOL 30. Because the infant continued to require platelet transfusions, the treating team switched back to the CTA hemofilter. The PMMA membrane retrieved at that exchange was examined by SEM, and representative images are shown in Supplementary Figure S1. Because corresponding pump tubing was unavailable, the PMMA specimen was excluded from the main three-circuit SEM comparison.

Because thrombocytopenia and recurrent circuit clotting persisted, a polyarylethersulfone (PAES) hemofilter (HF20; Vantive Co., Ltd., Tokyo, Japan) was subsequently introduced using the Prismaflex system (Vantive Co., Ltd., Tokyo, Japan). CKRT was then performed using combined pre- and post-dilution, with replacement fluid administered through both the pre-blood-pump (PBP) line and the post-dilution port.

An illustrative platelet time course was 65 × 10^9/L on the morning of DOL 31 and 26 × 10^9/L that afternoon. A platelet transfusion entry with a prescribed volume of 70 mL followed that evening and extended into DOL 32; the next morning, the platelet count was 139 × 10^9/L. The post-transfusion sample was obtained during routine care. Available blood-product records, including recorded volumes, infusion rates, and prescribed infusion durations for platelet concentrates, red blood cell products, and fresh frozen plasma, are summarized in Supplementary Table S1. Repeated and revised entries were consolidated to avoid double counting. Recorded volumes were not assumed to represent independently verified final delivered volumes.

A complete, consistently classified census of circuits and completed transfusions could not be reconstructed. Consequently, condition-specific median circuit lifespan, platelet transfusions per circuit-day, and on- versus off-CKRT transfusion rates were not calculated from the incomplete records.

2.5. Circuit Selection for SEM

Three clinically used CKRT circuits were selected for scanning electron microscopy (SEM) evaluation (Table 3). Circuit A used a CTA hemofilter (UT-03 Seco) with the ACH-Σ system under post-dilution conditions. Circuits B and C used PAES hemofilters (HF20) with the Prismaflex system under combined pre- and post-dilution conditions, with PBP flow rates of 100 and 300 mL/h, respectively.

Circuits A–C were intentionally selected to observe different treatment conditions; sampling was neither randomized nor consecutive. Their durations were 5 h 30 min, 6 h 40 min, and 7 h 53 min, respectively. According to the treating team's recollection, these circuits were stopped after pressure alarms reached the operative limits and treatment could not be continued. The exact alarm responsible for each termination and the corresponding pressure traces were not available. We therefore cannot distinguish filter clotting from other causes of pressure elevation in each circuit.

A circuit operated with a PBP rate of 200 mL/h was not recovered for SEM. Recurrent clotting had not been anticipated at the outset, and systematic collection of every circuit had not been established. The intentionally selected short-duration circuits should therefore not be taken as representative of all circuits used during the clinical course.

Table 3A lists the confirmed operating settings, and Table 3B summarizes routine morning laboratory results by DOL. The available laboratory results and transfusion records could not be reliably linked to the start and duration of each SEM circuit; therefore, circuit-specific laboratory values and transfusions are not reported. Filtration fraction was not calculated because hematocrit at the start of each circuit could not be verified. Patient net fluid removal is distinguished from nominal membrane ultrafiltration.

2.6. Other Clinical Course and Outcome

Respiratory function improved as generalized and pulmonary edema resolved. The infant was extubated on DOL 12, subsequently received high-flow nasal cannula therapy and low-flow supplemental oxygen, and was free from respiratory support by DOL 18. Enteral feeding was initiated on DOL 9 and gradually advanced.

Electroencephalography showed no definite epileptiform abnormalities. Brain magnetic resonance imaging performed on DOL 24 showed cerebral atrophy without other major abnormalities attributable to hypoxic–ischemic injury. Hypertension developed during the clinical course and required continuous nicardipine infusion followed by oral nifedipine. Erythropoietin and oral iron were administered for suspected renal anemia.

Kidney recovery was not achieved during the observation period, and the infant remained anuric and dependent on CKRT. Because prolonged extracorporeal therapy was complicated by recurrent circuit clotting, persistent thrombocytopenia, and repeated platelet transfusions, transition to peritoneal dialysis was considered.

On DOL 38, the infant was transferred to a specialized pediatric center for further kidney replacement therapy and possible PD initiation because anuria persisted and long-term dialysis appeared necessary. The local capacity for ongoing neonatal PD management and family training also informed transfer. No additional information was available on PD initiation, subsequent urine output, kidney recovery, or long-term outcome after transfer.

3. Materials and Methods

At circuit exchange, blood was not routinely returned to the patient by saline rinseback. Instead, blood from the used circuit was displaced with air and transferred into the new circuit for reuse. The retrieved specimens were not rinsed with saline before fixation. Specimen fixation was performed by the first author and initiated within approximately 1 h of circuit termination. The exact removal-to-fixation interval for each specimen was not recorded. Air displacement and residual ex vivo blood exposure may themselves have affected retention and morphology of loosely adherent material.

For all hemofilters, the housing was opened on the red blood-inlet side at a cut just above the label. Hollow fibers were taken from the radial center of the fiber bundle at the inlet-side sampling region. Thus, "central" refers to the center of the bundle cross-section, not the middle of the fiber length. Inlet, middle, and outlet segments were not systematically compared. Pump-tubing specimens were taken from the inner surface of the segment that had contacted the pump rollers on each platform.

On Prismaflex, PBP fluid enters upstream of the blood pump; consequently, the sampled pump segment in B and C carried prediluted blood. The pump segment in A carried blood before post-filter replacement. The sampling location was comparable in its roller-contact function, but dilution at that location and platform-specific tubing material were not controlled.

Specimens were fixed in 2.5% glutaraldehyde, washed with 0.1 M phosphate buffer (pH 7.4), post-fixed in 1% osmium tetroxide, washed again with phosphate buffer, and dehydrated through a graded ethanol series. The absence of saline rinsing before fixation is distinct from these subsequent buffer-washing steps. Unused PAES (HF20) and PMMA (CH-0.3W) membrane specimens were processed using the same specimen-preparation protocol as the used specimens and examined as morphological references (see Supplementary Figure S1 for the unused PMMA membrane). Unused CTA membrane and pump-tubing controls from either platform were unavailable.

After dehydration, the hollow-fiber and pump-tubing samples were washed twice with tert-butyl alcohol for 20 min each, frozen at −20 °C for 1–2 h, and dried using a vacuum freeze-drying system (VFD-20; Vacuum Device Inc., Ibaraki, Japan). The dried

specimens were mounted on metal specimen stages using conductive resin (DOTITE®; ThreeBond Fine Chemical Co., Ltd., Tokyo, Japan) and coated with platinum using an ion sputter coater (E-1030; Hitachi, Tokyo, Japan).

SEM observation was performed using an SU-3900 scanning electron microscope (Hitachi, Tokyo, Japan) at an accelerating voltage of 5–8 kV. The beam diameter, focus, and magnification were adjusted as required, and multiple areas of the hollow-fiber membranes and luminal surfaces of selected pump-tubing segments were examined to assess surface morphology and adherent components.

Two investigators evaluated the SEM findings qualitatively while aware of the circuit conditions. Representative images were chosen by consensus. Only a few images were retained as records, and the total number of fields examined per specimen was not documented. No prespecified random-field sampling, blinded grading, surface-area measurement, cellular count, or fibrin-density assessment was performed. Retrospective analysis of selected retained images would not remove the original selection bias.

Cellular and filamentous deposits were designated as blood cell-like or erythrocyte-like structures, platelet-like aggregates, and fibrin-like networks solely on morphology. Immunostaining, immunoelectron microscopy, or other confirmatory identification of platelets and fibrin was not performed.

4. SEM Findings

Representative retained images from the three principal circuits are described in Figure 2. The CTA hollow-fiber overview was obtained at ×500, whereas PAES overviews were obtained at ×300. Matched overview magnifications could not be recovered. Accordingly, the overview images were used to illustrate morphology and distribution within each specimen, not to measure or rank the extent of deposition between circuits.

In circuit A, the retained hollow-fiber images showed numerous adherent cellular structures, platelet-like aggregates, and filamentous fibrin-like networks. Filamentous deposits and focal aggregates were also present on the luminal pump-tubing surface.

In circuit B, the retained hollow-fiber images showed scattered cellular structures and platelet-like aggregates with localized filamentous material. Deposits were also observed on the sampled pump-tubing surface.

In circuit C, adherent structures appeared relatively sparse and localized in the retained hollow-fiber and pump-tubing images. This qualitative impression applies only to the selected images. Different overview magnifications, unblinded field selection, lack of quantitative analysis, and differences in exposure and clinical conditions preclude a validated ranking of total surface deposition.

The observed structures were not immunologically confirmed. The images document morphological appearances and do not demonstrate platelet activation, fibrin composition, total thrombus burden, or the mechanism of circuit termination.

Representative images of the unused PAES membrane are shown in Figure 3 as a reference for native luminal surface morphology. These images provide a reference for the PAES specimens only.

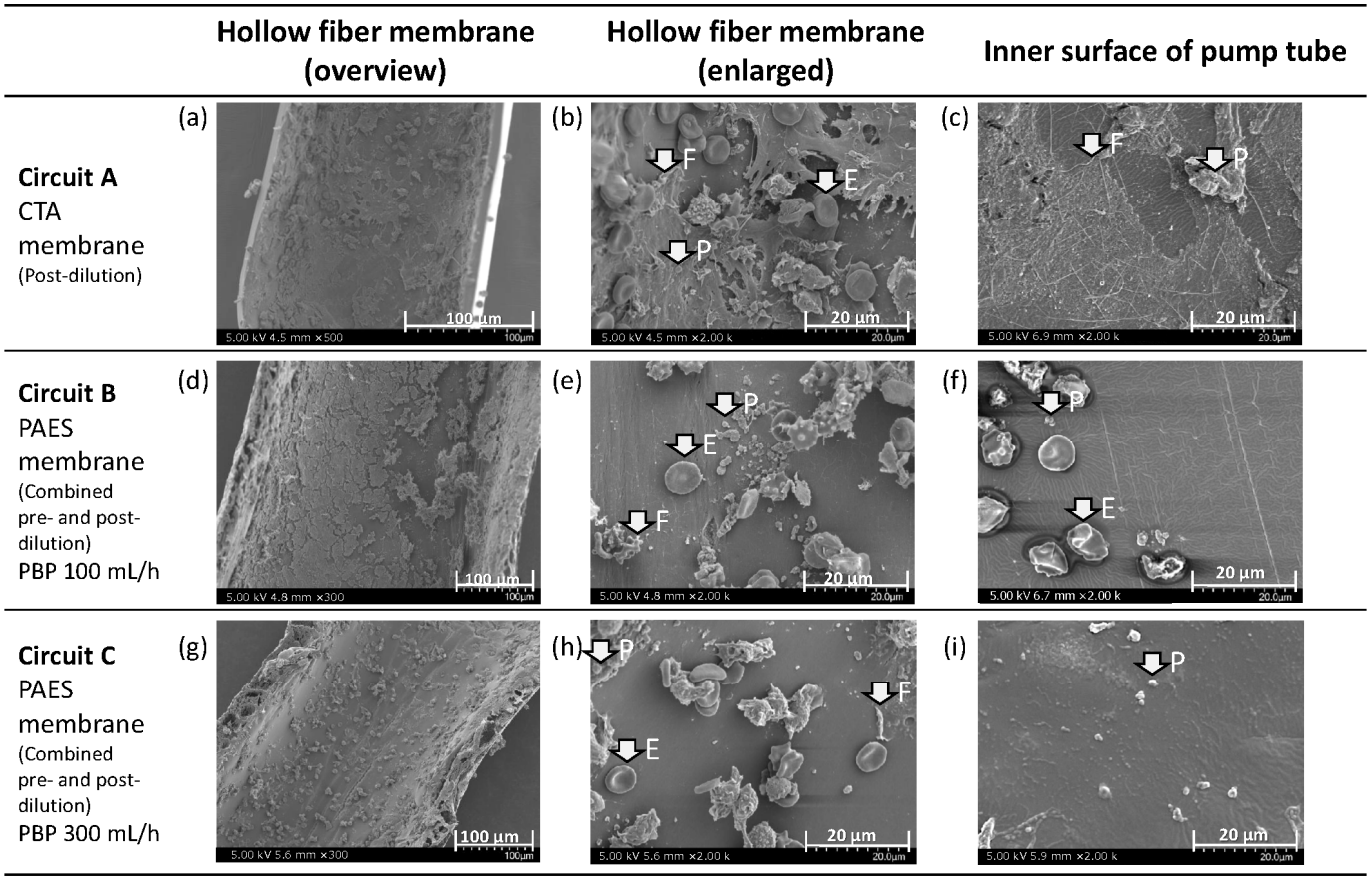


Figure 2. Representative scanning electron microscopy images of hollow-fiber membranes and the inner surfaces of blood-pump tubing from three neonatal CKRT circuits. Panels (a–c) show Circuit A (CTA membrane, post-dilution; circuit duration, 5 h 30 min); panels (d–f) show Circuit B (PAES membrane, combined pre- and post-dilution with PBP flow of 100 mL/h; circuit duration, 6 h 40 min); and panels (g–i) show Circuit C (PAES membrane, combined pre- and post-dilution with PBP flow of 300 mL/h; circuit duration, 7 h 53 min). The left column shows overview images of the hollow-fiber luminal surfaces, the middle column shows higher-magnification images of these surfaces, and the right column shows the inner surfaces of the roller-contact segments of the blood-pump tubing. Arrows identify representative erythrocyte-like structures (E), platelet-like aggregates (P), and fibrin-like networks (F). These designations are based solely on morphological appearance; their identities were not confirmed by specific staining or immunoelectron microscopy. Labels indicate selected examples rather than all visible structures. Overview images were acquired at ×500 for Circuit A (**a**) and ×300 for Circuits B and C (d,g); these images therefore do not permit direct comparison of the extent of deposition across circuits. All images in the middle and right columns were acquired at ×2000. Scale bars: 100 µm in (a,d,g); 20 µm in (b,c,e,f,h,i). Representative fields were selected by consensus of two investigators who were aware of the circuit conditions. The images provide descriptive morphological observations and were not subjected to quantitative analysis. CKRT, continuous kidney replacement therapy; CTA, cellulose triacetate; PAES, polyarylethersulfone; PBP, pre-blood pump.

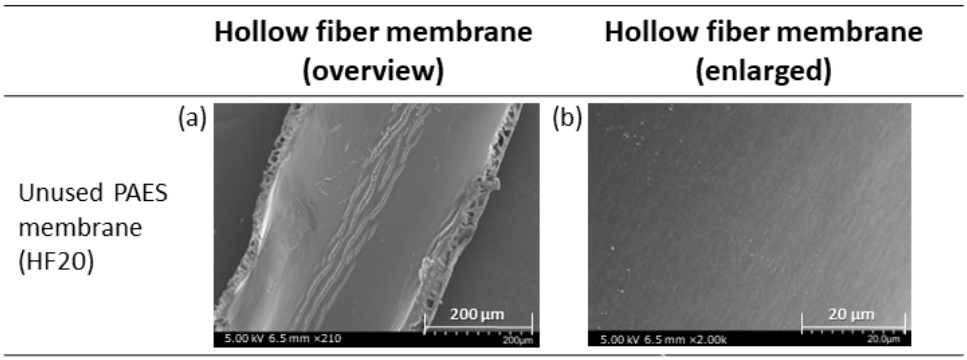


Figure 3. Scanning electron microscopy images of an unused PAES hollow-fiber membrane (HF20). (a) Overview of the hollow-fiber luminal surface at ×210. (b) Higher-magnification view of the luminal surface at ×2000. The unused membrane was processed using the same specimen-preparation protocol as the used membranes shown in Figure 2. The overview magnification differs from that of the used PAES membranes in Figure 2 (×300); direct comparison of surface coverage between these overview images is therefore inappropriate. Scale bars: (a) 200 µm; (b) 20 µm. These images provide a morphological reference for the PAES membrane only; unused CTA membrane and pump-tubing controls were unavailable. PAES, polyarylethersulfone; CTA, cellulose triacetate.

5. Discussion

This case illustrates the difficulties of prolonged CKRT in a critically ill neonate with severe birth asphyxia, DIC, persistent anuria, recurrent circuit pressure alarms, and thrombocytopenia requiring transfusions. SEM provided a descriptive record of adherent structures on retrieved membranes and pump tubing. Because several treatment and patient factors changed together, the observations cannot establish which factor accounted for the different appearances.

Small circulating blood volume, relatively large extracorporeal volume, low blood flow, and vascular-access limitations complicate neonatal CKRT [4,9]. Recent pediatric and young-adult CKRT data also highlight the clinical relevance of thrombocytopenia and early platelet decline [14]. Adult CKRT data associate platelet decline with kidney outcomes, but do not establish that the extracorporeal circuit causes thrombocytopenia [15]. In this infant, DIC, critical illness, changing coagulation status, and repeated transfusions remained competing explanations. Earlier adult CKRT cohorts also reported platelet decreases during treatment, although those observations cannot be directly extrapolated to neonates [16].

Platelet counts appeared to be better maintained during some CKRT interruptions. Blood samples were collected during routine care, without paired pre- and post-filter measurements or prespecified sampling times relative to CKRT initiation, interruption, or transfusion. This variability in sampling time limits interpretation of the observed post-transfusion increase in platelet count. Moreover, improvement in the initial DIC episode did not establish continuously normal coagulation: on DOL 37, fibrinogen was 145 mg/dL and aPTT was 44.7 s (1.55 times the recorded control). A contribution from the extracorporeal circuit remains possible but unproven.

Blood contact with artificial surfaces can promote protein adsorption and cellular adhesion. Experimental membrane studies support interactions between adsorbed fibrinogen and platelet or neutrophil receptors, and used-filter studies document adsorbed proteins and cells [11,17]. These findings provide a biological context for the observed morphology. They do not establish the identity of individual deposits in this case. Native membrane topography also differs by material, making unused membrane controls important; the absence of unused tubing controls further limits interpretation of the tubing appearances. Hemodialysis-associated platelet responses have also been described in the

broader dialysis literature; their magnitude depends on membrane and patient factors, and evidence from adult maintenance dialysis does not establish the mechanism in this neonate [18].

Predilution lowers blood cell and plasma protein concentrations at the filter inlet and may influence interactions between blood components and circuit surfaces. Previous studies have examined blood cell responses and circuit lifespan under different dilution modes [12,19]. In a prospective cohort of adults receiving CVVHDF without anticoagulation, combined pre- and post-dilution was associated with longer circuit lifespan than either mode alone [20]. The applicability of this finding to neonatal CKRT with nafamostat remains uncertain. In the present case, Circuits B and C differed in both PBP and post-filter replacement flow, resulting in different nominal membrane ultrafiltration rates despite identical net patient fluid removal (Table 3A). PBP flow alone was therefore insufficient to infer differences in filtration fraction or outlet hemoconcentration.

The site of nafamostat infusion and the dose delivered upstream of the filter differed between Circuit A and Circuits B and C. Although all three sampled circuits received 1.3 mg/h, only 1.0 mg/h was delivered before the filter in A, with 0.3 mg/h entering at the downstream venous chamber. In B and C, the full 1.3 mg/h entered between the blood pump and the filter. Thus, an equal total dose did not mean identical filter exposure. Nafamostat was not infused through the PBP line, and its delivery site was the same in B and C. Differences in blood dilution and plasma composition could nevertheless affect local anticoagulant concentration; this was not measured.

Circuit C ran 1 h 13 min longer than Circuit B and 2 h 23 min longer than Circuit A. Despite its longer run time, adherent structures appeared relatively sparse in the selected SEM images from Circuit C. Differences in platelet counts, coagulation status, and transfusion exposure, as well as specimen handling, field selection, and uneven deposition, may have influenced the appearance of these images. The difference between the selected images from Circuits B and C is hypothesis-generating. A protective effect of a PBP flow rate of 300 mL/h and a dose–response relationship remain undetermined.

Tubing findings require separate consideration. The roller-contact segment in B and C received PBP-diluted blood, whereas A had no upstream replacement flow. The platforms also used different tubing components, and native unused tubing was not examined. Differences on these surfaces therefore cannot be attributed to membrane material. Similarly, inlet-side fiber sampling does not characterize the outlet region, where intrafilter concentration may differ, or the full longitudinal distribution of deposits.

PD is an established option for neonatal AKI, and anticipated kidney recovery alone is not a contraindication [1,6]. Initial use of CKRT in this case reflected clinical priorities and local practice. Later persistent anuria prompted consideration of PD and transfer. Infant-specific extracorporeal systems such as CARPEDIEM and NIDUS offer approaches to the volume and fluid-control constraints of small infants, but were not locally available [7,8].

Registry comparisons have examined infant-specific CARPEDIEM treatment alongside adapted adult platforms, but differences between cohorts and treatment eras limit causal interpretation [21]. More recent French registry data in preterm and low-birthweight neonates support technical feasibility while documenting continuing complications, including thrombocytopenia and hypotension [22]. These populations and treatment settings differ from the present term neonate.

Heparin and regional citrate are alternative approaches to CKRT anticoagulation, with different monitoring and bleeding considerations [4,13]. The institutional choice of nafamostat reflected local practice and concern about hemorrhage. Citrate use for CKRT anticoagulation is off-label in Japan [13], and regional citrate anticoagulation was not

available at our institution. This report does not compare anticoagulants or establish a superior strategy for neonatal circuit patency.

Persistent anuria after severe asphyxia and DIC also requires consideration of irreversible parenchymal injury, cortical necrosis, and renal vascular thrombosis. Preserved renal blood flow in the clinical ultrasound notes does not definitively exclude these diagnoses. Absence of a verified detailed Doppler assessment or definitive pathological diagnosis limits etiological certainty. The lack of post-transfer information also prevents conclusions about subsequent PD use or kidney recovery.

Interruptions of CKRT can compromise delivered therapy and azotemic control [23]. In this case, blood from used circuits was often transferred to new circuits, so circuit termination should not automatically be equated with loss of the full extracorporeal blood volume. Available records did not permit a reliable condition-specific lifespan comparison or a transfusion-per-circuit-day analysis.

5.1. Limitations

This is a single-patient report involving three intentionally selected, short-duration circuits. There was no randomization, consecutive specimen collection, or control of membrane, platform, dilution, total filtration, anticoagulant exposure, blood-contact duration, or time-dependent illness. Exact termination alarms and pressure traces were unavailable, and circuit-specific start-of-run laboratory values and transfusions could not be verified. Complete clinical circuit and transfusion denominators were also unavailable.

The SEM assessment was unblinded and qualitative, with only selected images retained and no recorded total field count. Overview magnifications differed, and no quantitative coverage, cell count, or deposit-density measure was obtained. Deposit identification was morphological without confirmatory staining. Fiber sampling was confined to the radial center of the inlet-side region; unused CTA membrane and pump-tubing controls were unavailable, and systematic inlet-to-outlet sampling was not performed. Air-mediated blood transfer and variable blood-product priming may have influenced the retained deposits. Although fixation was initiated within approximately 1 h of circuit termination, exact removal-to-fixation intervals were not recorded, limiting assessment of any effects of fixation timing on deposit morphology. The additional PMMA membrane lacked matching tubing, and the 200-mL/h PBP circuit was not recovered. Long-term kidney outcome was unavailable.

5.2. Key Learning Points

First, interpretation of circuit morphology requires the treatment context, including net patient fluid removal, replacement distribution, anticoagulant delivery sites, access problems, exposure time, and clinical status. Second, equal total anticoagulant dose does not ensure equal upstream filter exposure. Third, representative SEM images can suggest research questions but cannot establish deposit identity, a membrane advantage, a dilution dose response, or causation of thrombocytopenia. Future studies should combine complete circuit and transfusion records with unused controls, standardized sampling and handling, and blinded assessment of prespecified fields.

6. Conclusions

During prolonged neonatal CKRT, the infant experienced recurrent circuit clotting, circuit pressure alarms, and persistent thrombocytopenia requiring repeated platelet transfusions. Qualitative SEM of retrieved hollow-fiber membranes and pump tubing showed blood cell-like structures, platelet-like aggregates, and fibrin-like networks. Adherent structures appeared relatively sparse in selected images from Circuit C (PAES membrane, PBP flow of 300 mL/h), which had the longest run time of the three examined

circuits. Treatment conditions and the infant's clinical status varied across circuits, limiting attribution of this observation to a specific membrane, platform, or dilution setting. These observations support further investigation of how replacement-fluid distribution and anticoagulant delivery relate to the morphology of circuit deposits during neonatal CKRT.

Supplementary Materials: The following supporting information can be downloaded at https://www.mdpi.com/article/10.3390/kidneydial6040074/s1: Table S1: Recorded blood-product volumes and infusion settings by day of life; Figure S1: Scanning electron microscopy images of unused and clinically used PMMA hollow-fiber membranes (CH-0.3W). The records in Table S1 do not constitute a complete circuit census or verified delivered transfusion totals.

Author Contributions: Conceptualization, A.T., M.Y. and S.A.; methodology, A.T., M.S. and M.Y.; investigation, A.T., M.S., S.T., T.I., T.Y., H.K., Y.M., K.N. and M.Y.; scanning electron microscopy observation and qualitative image evaluation, A.T. and M.S.; data curation, A.T.; formal analysis, A.T. and M.Y.; visualization, A.T. and M.Y.; writing—original draft preparation, A.T.; writing—review and editing, M.S., S.T., T.I., T.Y., H.K., Y.M., K.N., M.Y., K.S. and S.A.; supervision, K.S. and S.A.; project administration, A.T. All authors have read and agreed to the published version of the manuscript.

Funding: This research received no external funding. The article processing charge (APC) will be paid by the authors.

Institutional Review Board Statement: The study was conducted in accordance with the Declaration of Helsinki and approved by the Ethics Committee of Kindai University Hospital (approval No. R05-188; date of approval: 19 February 2024).

Informed Consent Statement: Written informed consent for the academic use and publication of clinical information was obtained from the patient's legal guardians as part of the institution's comprehensive consent process.

Data Availability Statement: The data supporting the findings of this study were obtained from patient medical records and are not publicly available due to ethical and privacy restrictions. Portions of the analyzed data are included within this article. Additional data may be made available from the corresponding author upon reasonable request and with permission from the Ethics Committee of Kindai University Hospital.

Acknowledgments: The authors thank the clinical engineering staff and medical staff of Kindai University Hospital for their support in CKRT management and sample collection. The authors also thank Masami Takeichi of the Center for Morphological Analyses, Core Research Facilities, Kindai University Faculty of Medicine, for technical guidance and support with scanning electron microscopy. ChatGPT (GPT-5; OpenAI) was used for English language editing of this manuscript. The authors take full responsibility for the accuracy, interpretation, and final content of the manuscript.

Conflicts of Interest: S.A. has received honoraria from Daiichi Sankyo, Mitsubishi Tanabe Pharma, Kyowa Kirin, Novartis, and Otsuka Pharmaceutical. The other authors declare no conflicts of interest.

References

1. Coleman, C.; Tambay Perez, A.; Selewski, D.T.; Steflik, H.J. Neonatal acute kidney injury. *Front. Pediatr.* **2022**, *10*, 842544. https://doi.org/10.3389/fped.2022.842544.
2. Kirkley, M.J.; Boohaker, L.; Griffin, R.; Soranno, D.E.; Gien, J.; Askenazi, D.; Gist, K.M.; Neonatal Kidney Collaborative. Acute kidney injury in neonatal encephalopathy: An evaluation of the AWAKEN database. *Pediatr. Nephrol.* **2019**, *34*, 169–176. Correction in *Pediatr. Nephrol.* **2019**, *34*, 363. https://doi.org/10.1007/s00467-018-4068-2.

3. Sweetman, D.U.; Onwuneme, C.; Watson, W.R.; O'Neill, A.; Murphy, J.F.A.; Molloy, E.J. Renal function and novel urinary biomarkers in infants with neonatal encephalopathy. *Acta Paediatr.* **2016**, *105*, e513–e519. https://doi.org/10.1111/apa.13555.
4. Cortina, G.; Daverio, M.; Demirkol, D.; Chanchlani, R.; Deep, A. Continuous renal replacement therapy in neonates and children: What does the pediatrician need to know? An overview from the Critical Care Nephrology Section of the European Society of Paediatric and Neonatal Intensive Care (ESPNIC). *Eur. J. Pediatr.* **2024**, *183*, 529–541. https://doi.org/10.1007/s00431-023-05318-0.
5. Yoshioka, M.; Todo, A.; Masuda, Y.; Nakano, K.; Sakaguchi, M.; Arima, S. Clinical experience and future challenges in CKRT implementation for acute kidney injury following neonatal asphyxia. *J. Jpn. Soc. Blood Purif. Crit. Care* **2025**, *16*, 74–79. https://doi.org/10.34325/jsbpcc.16.2_74. (In Japanese)
6. Nourse, P.; Cullis, B.; Finkelstein, F.; Numanoglu, A.; Warady, B.; Antwi, S.; McCulloch, M. ISPD guidelines for peritoneal dialysis in acute kidney injury: 2020 Update (paediatrics). *Perit. Dial. Int.* **2021**, *41*, 139–157. https://doi.org/10.1177/0896860820982120.
7. Battista, J.; De Luca, D.; Eleni Dit Trolli, S.; Allard, L.; Bacchetta, J.; Bouhamri, N.; Enoch, C.; Faudeux, C.; Guichoux, J.; Javouhey, E.; et al. CARPEDIEM® for continuous kidney replacement therapy in neonates and small infants: A French multicenter retrospective study. *Pediatr. Nephrol.* **2023**, *38*, 2827–2837. https://doi.org/10.1007/s00467-022-05871-0.
8. Lambert, H.; Hiu, S.; Coulthard, M.G.; Matthews, J.N.S.; Holstein, E.-M.; Crosier, J.; Agbeko, R.; Brick, T.; Duncan, H.; Grant, D.; et al. The Infant KIdney Dialysis and Utrafiltration (I-KID) Study: A stepped-wedge cluster-randomized study in infants, comparing peritoneal dialysis, continuous venovenous hemofiltration, and Newcastle Infant Dialysis Ultrafiltration System, a novel infant hemodialysis device. *Pediatr. Crit. Care Med.* **2023**, *24*, 604–613. https://doi.org/10.1097/PCC.0000000000003220.
9. Hackbarth, R.; Bunchman, T.E.; Chua, A.N.; Somers, M.J.; Baum, M.; Symons, J.M.; Brophy, P.D.; Blowey, D.; Fortenberry, J.D.; Chand, D.; et al. The effect of vascular access location and size on circuit survival in pediatric continuous renal replacement therapy: A report from the PPCRRT Registry. *Int. J. Artif. Organs* **2007**, *30*, 1116–1121. https://doi.org/10.1177/039139880703001212.
10. Bonomini, M.; Piscitani, L.; Di Liberato, L.; Sirolli, V. Biocompatibility of surface-modified membranes for chronic hemodialysis therapy. *Biomedicines* **2022**, *10*, 844. https://doi.org/10.3390/biomedicines10040844.
11. Michikoshi, J.; Matsumoto, S.; Miyawaki, H.; Morita, M.; Niu, H.; Seo, K.; Hagiwara, S.; Kitano, T. Evaluation of proteins and cells that adsorb to dialysis membranes used in continuous hemodiafiltration: Comparison of AN69ST, polymethylmethacrylate, and polysulfone membranes. *Blood Purif.* **2019**, *48*, 358–367. https://doi.org/10.1159/000501632.
12. Sakurai, K.; Saito, T.; Yamauchi, F.; Asahi, D.; Hosoya, H. Comparison of the effects of predilution and postdilution hemodiafiltration on neutrophils, lymphocytes and platelets. *J. Artif. Organs* **2013**, *16*, 316–321. https://doi.org/10.1007/s10047-013-0698-0.
13. Doi, K.; Nishida, O.; Shigematsu, T.; Sadahiro, T.; Itami, N.; Iseki, K.; Yuzawa, Y.; Okada, H.; Koya, D.; Kiyomoto, H.; et al. The Japanese Clinical Practice Guideline for acute kidney injury 2016. *J. Intensive Care* **2018**, *6*, 48. https://doi.org/10.1186/s40560-018-0308-6.
14. Basalely, A.; Gist, K.M.; Stanski, N.L.; Fuhrman, D.Y.; Seo, J.; Ollberding, N.J.; Strong, A.; Damian, M.; Morgan, C.; Reynaud, S.; et al. Thrombocytopenia in children and young adults undergoing continuous renal replacement therapy: A WE-ROCK study. *Blood Purif.* **2025**, *54*, 322–333. https://doi.org/10.1159/000545777.
15. Griffin, B.R.; Ten Eyck, P.; Faubel, S.; Jalal, D.; Gallagher, M.; Bellomo, R. Platelet decreases following continuous renal replacement therapy initiation as a novel risk factor for renal nonrecovery. *Blood Purif.* **2022**, *51*, 559–566. https://doi.org/10.1159/000517232.
16. Ferreira, J.A.; Johnson, D.W. The incidence of thrombocytopenia associated with continuous renal replacement therapy in critically ill patients. *Ren. Fail.* **2015**, *37*, 1232–1236. https://doi.org/10.3109/0886022X.2015.1057799.
17. Koga, Y.; Fujieda, H.; Meguro, H.; Ueno, Y.; Aoki, T.; Miwa, K.; Kainoh, M. Biocompatibility of polysulfone hemodialysis membranes and its mechanisms: Involvement of fibrinogen and its integrin receptors in activation of platelets and neutrophils. *Artif. Organs* **2018**, *42*, E246–E258. https://doi.org/10.1111/aor.13268.
18. Daugirdas, J.T.; Bernardo, A.A. Hemodialysis effect on platelet count and function and hemodialysis-associated thrombocytopenia. *Kidney Int.* **2012**, *82*, 147–157. https://doi.org/10.1038/ki.2012.130.
19. Uchino, S.; Fealy, N.; Baldwin, I.; Morimatsu, H.; Bellomo, R. Pre-dilution vs. post-dilution during continuous veno-venous hemofiltration: Impact on filter life and azotemic control. *Nephron Clin. Pract.* **2003**, *94*, c94–c98. https://doi.org/10.1159/000072492.

20. Wang, F.; Zhang, M.; Li, X.; Sun, X.; He, X.; Guan, M.; Chen, Z.; Lin, L.; Tang, X.; Zhang, L. An evaluation of different dilution modes on circuit lifespan during continuous veno-venous hemodiafiltration without anticoagulation. *Semin. Dial.* **2024**, *37*, 52–58. https://doi.org/10.1111/sdi.13147.

21. Goldstein, S.L.; Vidal, E.; Ricci, Z.; Paglialonga, F.; Peruzzi, L.; Giordano, M.; Laforgia, N.; Ronco, C. Survival of infants treated with CKRT: Comparing adapted adult platforms with the Carpediem™. *Pediatr. Nephrol.* **2022**, *37*, 667–675. Correction in *Pediatr. Nephrol.* **2022**, *37*, 689. https://doi.org/10.1007/s00467-021-05180-y.
22. Battista, J.; Eleni Dit Trolli, S.; Ranchin, B.; Bacchetta, J.; Baleine, J.F.; De Luca, D.; Decramer, S.; Enoch, C.; Faudeux, C.; Fila, M.; et al. Continuous kidney replacement therapy with CARPEDIEM® of premature and low birth weight neonates from the French registry. *Pediatr. Nephrol.* **2026**, *41*, 1829–1837. https://doi.org/10.1007/s00467-025-06896-x.
23. Uchino, S.; Fealy, N.; Baldwin, I.; Morimatsu, H.; Bellomo, R. Continuous is not continuous: The incidence and impact of circuit "down-time" on uraemic control during continuous veno-venous haemofiltration. *Intensive Care Med.* **2003**, *29*, 575–578. https://doi.org/10.1007/s00134-003-1672-8.

Disclaimer/Publisher's Note: The statements, opinions and data contained in all publications are solely those of the individual author(s) and contributor(s) and not of MDPI and/or the editor(s). MDPI and/or the editor(s) disclaim responsibility for any injury to people or property resulting from any ideas, methods, instructions or products referred to in the content.